

# Phase Relations in the $\text{Ag}_8\text{SiS}_6$ - $\text{Ag}_8\text{SiSe}_6$ System and Characterization of Solid Solutions

Albina Poladova<sup>1\*</sup> , Aynura Yagubova<sup>2</sup> 

**Abstract.** Argyrodite-type compounds and the phases derived from them represent environmentally benign and valuable functional materials exhibiting a wide range of properties, including thermoelectric, photoelectric, and optical characteristics. In addition, these materials demonstrate ionic conductivity through  $\text{Cu}^+$  and  $\text{Ag}^+$  ions, which makes them promising candidates for application as electrode or electrolyte materials in ion-selective electrodes, various types of batteries, displays, and sensors. In this work, the phase equilibria of the  $\text{Ag}_8\text{SiS}_6$ – $\text{Ag}_8\text{SiSe}_6$  system were investigated using differential thermal analysis and X-ray diffraction methods, and the corresponding  $T$ – $x$  phase diagram was constructed. The system was found to be quasi-binary and is characterized by the formation of an extended region of solid solutions between the HT- $\text{Ag}_8\text{SiS}_6$  and HT- $\text{Ag}_8\text{SiSe}_6$  compounds. The polymorphic transition temperature of  $\text{Ag}_8\text{SiS}_6$  decreases with increasing formation of solid solutions. It was determined that at room temperature the homogeneity region of the  $\delta$ -phase extends within the composition range of 70–90 mol%  $\text{Ag}_8\text{SiSe}_6$ . Furthermore, the lattice parameters of the obtained solid solutions were calculated from X-ray diffraction data, revealing a linear dependence on composition.

**Keywords:** silver-silicon sulfide, silver-silicon selenide, argyrodite-like compounds, DTA, XRD, phase equilibria, polymorphic transformation

## Introduction

Binary and more complex chalcogenides formed by copper and silver with p-block elements are at the center of researchers' attention due to their thermoelectric, optical, photoelectric, and other functional properties (Khan, 2023; Puthran, 2024; Li, 2024; Portniagin, 2025). One of the important classes of these multicomponent materials is the argyrodite family compounds with the general formula  $\text{A}^I_8\text{B}^{\text{IV}}\text{X}_6$  ( $\text{A}^I$ -Cu, Ag;  $\text{B}^{\text{IV}}$ -Si, Ge, Sn; X-S, Se, Te) (Wang, 2024; Parashchuk, 2025; Ghata, 2025). A distinctive feature of argyrodite-type compounds is the occurrence of polymorphic phase transitions at comparatively low temperatures ( $\leq 530$  K). The low-temperature forms crystallize in ordered crystal structures with reduced symmetry, while the high-temperature modifications typically possess a cubic lattice structure (Kuhs, 1979; Bindi, 2018; Babanly, 2024).

These compounds are characterized by a rigid anion framework constructed from tetrahedrally coordinated  $[\text{SiX}_4]$  units ( $\text{X} = \text{S}, \text{Se}$ ) and a highly disordered sublattice of mobile  $\text{Ag}^+$  cations. Such a unique crystal structure results in high ionic conductivity as well as favorable optical, thermoelectric, and other physical properties.

<sup>1</sup> Institute of Chemistry, PhD student, Baku, Azerbaijan

<sup>2</sup> Baku State University, Master's student, Baku, Azerbaijan

\*Corresponding author. E-mail: [albinapoladova@gmail.com](mailto:albinapoladova@gmail.com)

Received: 7 January 2026; Accepted: 24 March 2026; Published online: 25 April 2026

© The Author(s) 2026. This is an open access article distributed under the terms of the Creative Commons Attribution-NonCommercial 4.0 International License (CC BY-NC 4.0).

Due to the structural features of their high-temperature phases, argyrodite compounds exhibit superionic conductivity, where copper and silver ions demonstrate high mobility, leading to large values of cationic conductivity and ionic diffusion in the solid state (Shen, 2023; Studenyak, 2020; Kang, 2026; Ren, 2023). These properties make such materials promising for applications as solid electrolytes, ion-selective electrodes, thermoelectric energy conversion materials, and components of photoelectric and optoelectronic devices (Lin, 2024; Wei, 2024; Dallas, 2025; Bustamante, 2025; Li, 2020). Due to these properties, argyrodite-based systems have been extensively studied by various research groups. In previous studies (Bayramova, 2022; Amiraslanova, 2023; Bayramova, 2023; Poladova, 2025; Huseynova, 2025; Ismayilova, 2025), phase equilibria and phase transitions in systems composed of argyrodite-type compounds were experimentally investigated. These studies revealed that such systems are typically characterized by the formation of wide or even unlimited substitutional solid solutions.

The objective of the present work was to examine the phase equilibria in the  $\text{Ag}_8\text{SiS}_6\text{--Ag}_8\text{SiSe}_6$  system in order to obtain new variable-composition phases based on silicon-containing argyrodites. The initial compounds forming this system have been previously studied in considerable detail.

The compound  $\text{Ag}_8\text{SiS}_6$  melts congruently at 1213 K (Gorochov, 1968), 1223 K (Boivin, 1967), 1232 K (Cambi, 1961), and 1243 K (Venkatraman, 1995), while its polymorphic transition temperature is reported as 507 K (Gorochov, 1968; Boivin, 1967) and 510 K (Venkatraman, 1995). The low-temperature modification of  $\text{Ag}_8\text{SiS}_6$  crystallizes in the orthorhombic system with the following lattice parameters: space group  $Pna2_1$ ,  $a = 1.5024$ ,  $b = 0.7428$ ,  $c = 1.0533$  nm (Krebs, 1977);  $a = 1.5043$ ,  $b = 0.7452$ ,  $c = 1.0565$  nm (Kuhs, 1979). The high-temperature modification has a cubic structure: space group  $F\bar{4}3m$ ,  $a = 1.063$  nm (Gorochov, 1968).

The compound  $\text{Ag}_8\text{SiSe}_6$  melts congruently at 1258 K (Venkatraman, 1995), 1278 K (Amiraslanova, 2023), 1203 K (Gorochov, 1968; Hofmann, 1988), 1268 K (Piskach, 2006), and its polymorphic transition temperature is reported as 315 K (Amiraslanova, 2023) and 354 K (Amiraslanova, 2023). Three modifications have been reported for this compound (Liang, 2020; Gorochov, 1968; Hofmann, 1988; Heep, 2017). The high-temperature modification crystallizes in a face-centered cubic lattice (space group  $F\bar{4}3m$ ,  $a = 1.097$  nm (Gorochov, 1968; Hofmann, 1988),  $a = 1.09413(1)$  nm (Heep, 2017). The intermediate modification has a simple cubic structure (space group  $P2_13$  (Heep, 2017) or  $P4_232$ ,  $a = 1.087$  nm (Gorochov, 1968). The low-temperature modification crystallizes in a tetragonal structure (space group  $I\bar{4}m2$ ,  $a = 0.7706$ ,  $c = 1.10141$  nm (Gorochov, 1968; Hofmann, 1988). However, Jiang and co-authors (Jiang, 2020) reported that the powder X-ray diffraction pattern of LT- $\text{Ag}_8\text{SiSe}_6$  cannot be satisfactorily indexed using this structural model. The authors identified the presence of two different sets of reflections in the diffractogram and showed that most of the peaks can be indexed in the orthorhombic system with space group  $Pmn2_1$ . In addition, weak-intensity peaks observed in the angular regions of  $33.5^\circ$ ,  $34.7^\circ$ , and  $37.0^\circ$  were attributed to the orthorhombic RT- $\text{Ag}_2\text{Se}$  phase (Jiang, 2020).

## Materials and Methods

The initial compounds were synthesized by melting high-purity elements (at least 99.999 wt.% purity) Ag, Si, S, and Se in evacuated quartz ampoules. To prevent the reaction of silicon with the quartz ampoule, the inner surface of the ampoule was carbon-coated (graphitized) at the beginning of the process.

Due to the high vapor pressure of sulfur and selenium, the synthesis was performed in a two-zone regime in an inclined furnace. The temperature of the lower “hot zone” was set 50 K above the melting point of the compound, namely 1280 K for  $\text{Ag}_8\text{SiS}_6$  and 1300 K for  $\text{Ag}_8\text{SiSe}_6$ . The upper “cold zone” was heated to a temperature 50–100 K below the boiling point of the appropriate chalcogen. In the

cold zone, sulfur and selenium vapors condensed and returned to the reaction zone. After the main portion of the chalcogen had reacted, the ampoule was completely placed inside the furnace, kept for 2–3 hours, and then cooled to room temperature in the switched-off furnace.

The purity of the synthesized compounds was confirmed by differential thermal analysis (DTA) and X-ray diffraction (XRD). The obtained analytical results for both compounds were found to be in good agreement with previously reported literature data.

Alloys of the  $\text{Ag}_8\text{SiS}_6$ – $\text{Ag}_8\text{SiSe}_6$  system were synthesized by melting appropriate stoichiometric amounts of the pre-synthesized and well-characterized starting compounds. To achieve equilibrium, the samples were annealed at 800 K for an extended period (500 hours). Two series of samples for each composition were synthesized. The first series was furnace-cooled after thermal treatment (the furnace was switched off and the samples were allowed to cool gradually), whereas the second series was water-quenched from 800 K by rapidly immersing the ampoule in cold water. The synthesized samples were investigated using DTA and XRD methods.

Differential thermal analysis was performed using a NETZSCH 404 F1 Pegasus instrument and a multi-channel DTA device based on a “TC-08 Thermocouple Data Logger” with a temperature measurement accuracy of  $\pm 2$  K. The experimental data were processed using NETZSCH Proteus software. X-ray phase analysis was performed at room temperature in the  $2\theta$  range of  $5$ – $75^\circ$  using  $\text{CuK}\alpha_1$  radiation on a Bruker D2 PHASER diffractometer. The obtained diffraction patterns were analyzed with TOPAS V3.0 software, and the lattice parameters were subsequently determined.

## Results and Discussion

Both series of alloys in the  $\text{Ag}_8\text{SiS}_6$ – $\text{Ag}_8\text{SiSe}_6$  system were examined using differential thermal DTA and XRD techniques. The experimental results showed that complete mutual solubility exists between the high-temperature phases of the initial compounds in the  $\text{Ag}_8\text{SiS}_6$ – $\text{Ag}_8\text{SiSe}_6$  system. Based on their low-temperature modifications, wide solid solutions are formed. The resulting powder diffraction patterns are shown in Figure 1. It was established that the diffraction patterns of samples within the composition range of 70–90 mol%  $\text{Ag}_8\text{SiSe}_6$  correspond to a cubic system and qualitatively differ from those of the initial compounds. Samples containing 10–60 mol%  $\text{Ag}_8\text{SiSe}_6$  exhibit diffraction patterns identical to those of pure orthorhombic  $\text{Ag}_8\text{SiS}_6$ .

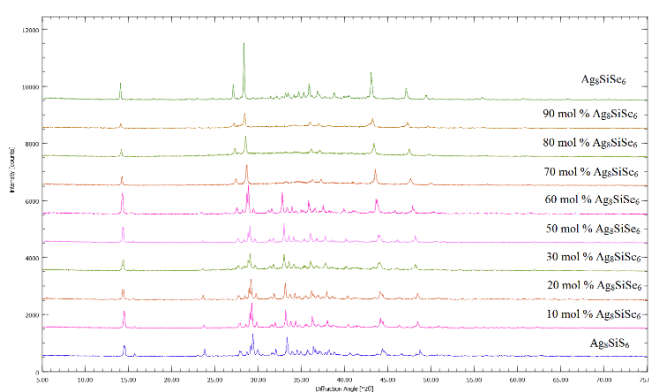


**Figure 1**

Powder X-ray diffraction patterns of selected alloys in the  $\text{Ag}_8\text{SiS}_6$ – $\text{Ag}_8\text{SiSe}_6$  system slowly cooled after annealing

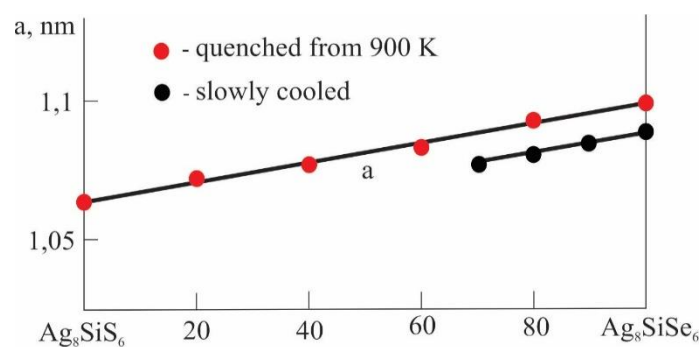
Thus, the results of the presented powder diffraction patterns indicate that, at room temperature, alloys containing 70–90 mol %  $\text{Ag}_8\text{SiSe}_6$  form cubic-structured phases ( $\delta$ -phase). The solubility in the RT- $\text{Ag}_8\text{SiS}_6$ -based phase exceeds 60 mol%, while the solubility in the RT- $\text{Ag}_8\text{SiSe}_6$ -based phase is below

10 mol%. In Table 1, the powder diffraction patterns of the initial compounds of the  $\text{Ag}_8\text{SiS}_6$ – $\text{Ag}_8\text{SiSe}_6$  system and of both series of alloys were indexed using the TOPAS V3.0 software and the lattice parameters were calculated. Figure 2 shows the concentration dependence of the cubic lattice parameter. As can be seen, the lattice parameter of both quenched and slowly cooled samples is a linear function of composition and follows Vegard's law. It should be noted that the lattice parameter values of the samples annealed at 800 K are slightly higher than those of the cubic phases measured at room temperature, which can be explained by the thermal expansion of the lattice upon heating.

**Table 1**Crystallographic parameters of phases in the  $\text{Ag}_8\text{SiS}_6$ – $\text{Ag}_8\text{SiSe}_6$  system

Composition, mol% $\text{Ag}_8\text{SiSe}_6$	Syngony, Sp.Gr., lattice parameters, nm	
	Slowly cooled alloys	Quenched from 800 K alloys
0 ( $\text{Ag}_8\text{SiS}_6$ )	Orthorhombic, ( $Pna2_1$ ): $A = 1.5032(3)$ , $b = 0.7430(2)$ , $c = 1.0538(3)$	Cubic, ( $F\bar{4}3m$ ): $a = 1.0635(3)$
10	"-, $a = 1.5146(4)$ ; $b = 0.749(3)$ ; $c = 1.0627(3)$	
20	"-, $a = 1.5146(4)$ ; $b = 0.749(3)$ ; $c = 1.0627(3)$	"-, $a = 1.0824(4)$
30	"-, $a = 1.5146(4)$ ; $b = 0.749(3)$ ; $c = 1.0627(3)$	"-, $a = 1.0915(4)$
50	"-, $a = 1.5146(4)$ ; $b = 0.749(3)$ ; $c = 1.0627(3)$	
60	"-, $a = 1.5146(4)$ ; $b = 0.749(3)$ ; $c = 1.0627(3)$	"-, $a = 1.1167(4)$
70	Cubic, ( $F\bar{4}3m$ ): $a = 1.077(3)$	
80	"-, $a = 1.081(4)$	"-, $a = 1.1344(3)$
90	"-, $a = 1.085(4)$	
100 ( $\text{Ag}_8\text{SiSe}_6$ )	Cubic, $P4_232$ , $a = 1.0891(3)$	"-, $a = 1.0965(3)$

On the basis of the DTA data (Table 2), the phase diagram of the system was constructed (Figure 4). As shown, the system exhibits quasi-binary behavior and is characterized by the formation of an extended region of solid solutions ( $\delta$ -phase) between HT- $\text{Ag}_8\text{SiS}_6$  and HT  $\text{Ag}_8\text{SiSe}_6$ . The temperatures along the liquidus and solidus lines vary monotonically between the melting points of the starting compounds.

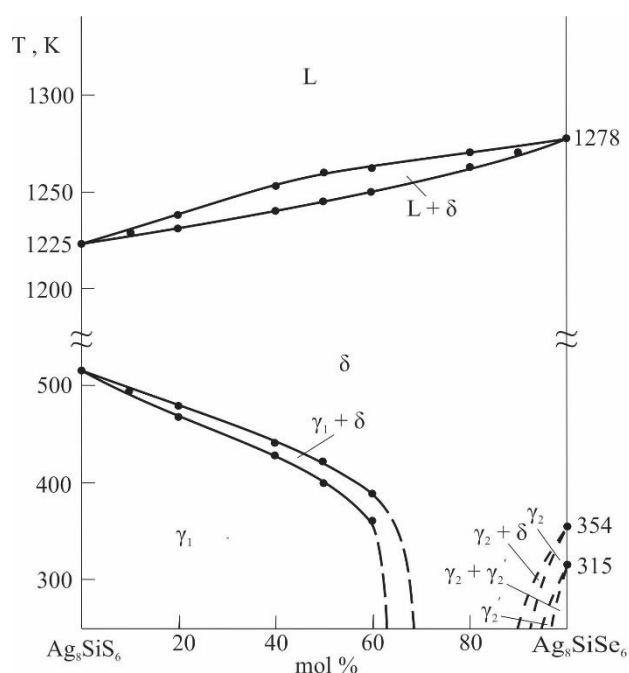
**Figure 2**Dependence of the cubic lattice parameter of the  $\text{Ag}_8\text{SiS}_6$ – $\text{Ag}_8\text{SiSe}_6$  system on composition

The DTA results show that the polymorphic phase transition characteristic of  $\text{Ag}_8\text{SiS}_6$  at 513 K shifts toward lower temperatures with  $\text{Ag}_8\text{SiSe}_6$  content. In alloys containing  $\geq 60$  mol %  $\text{Ag}_8\text{SiSe}_6$ , no thermal effects are observed on the DTA curves, indicating that the transition occurs below room temperature.

**Table 2**

The DTA results for the alloys of the  $\text{Ag}_8\text{SiS}_6$ - $\text{Ag}_8\text{SiSe}_6$  system

Composition, mol% $\text{Ag}_8\text{SiSe}_6$	Thermal effects, K
0 ( $\text{Ag}_8\text{SiS}_6$ )	513; 1225
10	495; 1238
20	467–482; 1232–1238
40	428–443; 1240–1253
50	400–424; 1245–1260
60	360–389; 1249–1262
80	1262–1271
90	1270
100 ( $\text{Ag}_8\text{SiSe}_6$ )	315; 354; 1278

**Figure 3**

Phase diagram of the  $\text{Ag}_8\text{SiS}_6$ - $\text{Ag}_8\text{SiSe}_6$  system

## Conclusion

This work presents new data on the phase equilibria in the  $\text{Ag}_8\text{SiS}_6$ - $\text{Ag}_8\text{SiSe}_6$  system obtained by differential thermal analysis (DTA) and X-ray diffraction (XRD). Based on the experimental results, the T-x phase diagram of the system was constructed. The system exhibits quasi-binary behavior and forms a continuous series of substitutional solid solutions between the high-temperature modifications of  $\text{Ag}_8\text{SiS}_6$  and  $\text{Ag}_8\text{SiSe}_6$ . The formation of these solid solutions results in a decrease in the polymorphic transition temperature of  $\text{Ag}_8\text{SiS}_6$ . As a consequence, the ion-conducting cubic phase becomes stabilized at room temperature and even below within the composition range of 70–

90 mol%  $\text{Ag}_8\text{SiSe}_6$ . The lattice parameters of the obtained solid solutions were calculated from powder X-ray diffraction data, and their compositional dependence was found to follow Vegard's law. The newly synthesized solid solutions are promising environmentally friendly materials that exhibit thermoelectric properties along with mixed ionic–electronic conductivity.

### Declaration of Competing Interests

The authors declare that they have no known competing financial interests or personal relationships that could have appeared to influence the work reported in this paper.

### References

1. Amiraslanova, A. J., Babanly, K. N., Imamaliyeva, S. Z., Akhmedov, E. I., Yusibov, Yu. A., & Babanly, M. B. (2023). Surfaces of crystallization and phase relations in the  $6\text{Ag}_2\text{Se}+\text{Ag}_8\text{SiTe}_6\leftrightarrow 6\text{Ag}_2\text{Te}+\text{Ag}_8\text{SiSe}_6$  reciprocal system. *Azerbaijan Chemical Journal*, (3). <https://doi.org/10.32737/0005-2531-2023-3-6-17>
2. Babanly, M. B., Yusibov, Y. A., Imamaliyeva, S. Z., Babanly, D. M., & Alverdiyev, I. J. (2024). Phase Diagrams in the Development of the Argyrodite Family Compounds and Solid Solutions Based on Them. *Journal of Phase Equilibria and Diffusion*, 45(3), 228–255. <https://doi.org/10.1007/s11669-024-01088-w>
3. Bayramova, U. R., Babanly, K. N., Mashadiyeva, L. F., Yusibov, Yu. A., & Babanly, M. B. (2023). Phase Equilibria in the  $\text{Cu}_2\text{Se}-\text{Cu}_8\text{SiSe}_6-\text{Cu}_8\text{GeSe}_6$  System. *Russian Journal of Inorganic Chemistry*, 68(11), 1611–1621. <https://doi.org/10.1134/S0036023623602027>
4. Bairamova, U. R., Poladova, A. N., & Mashadiyeva, L. F. (2022). Synthesis and x-ray study of the  $\text{Cu}_8\text{Ge}_{(1-x)}\text{Si}_x\text{S}_6$  solid solutions. *New Materials and Compounds Applied*, 6(3), 276–281.
5. Bindi, L., & Biagioni, C. (2018). A crystallographic excursion in the extraordinary world of minerals: the case of Cu- and Ag-rich sulfosalts. *Acta Crystallographica Section B: Structural Science, Crystal Engineering and Materials*, 74(6) 527–538. <https://doi.org/10.1107/S2052520618014452>
6. Boivin, J. -C., Thomas, D., & Tridot, G. (1967). Contribution a l'etude des Systèmes: sulfure de silicium et sulfure de cuivre ou d'argent. *Comptes Rendus des Séances de l'Académie des Sciences. Vie Académique*, 264(16), 1286–1289.
7. Bustamante, J., Ghata, A., Naik, A. A., Ertural, Ch., Ueltzen, K., Zeier, W. G., & George, J. (2025). Thermal Transport in  $\text{Ag}_8\text{TS}_6$  (T= Si, Ge, Sn) Argyrodites: An Integrated Experimental, Quantum-Chemical, and Computational Modelling Study. *arXiv*. <https://doi.org/10.48550/arXiv.2510.23133>
8. Cambi, L., & Elli, M. (1961). Sui sulfogermanati: argirodite sintetica. *Atti della Accademia Nazionale dei Lincei, Classe di Scienze Fisiche, Matematiche e Naturali, Rendiconti*, 30, 11–15.
9. Dallas, P., Tzitzios, V. K., Givalou, L., Tspas, P., Basinab, G., Sakellis, E., Boukos, N., & Stergiopoulos, T. (2025). Effects of ligand coordination on  $\text{Ag}_8\text{SnS}_6$  as a photoabsorber for thin film solar cells. *Journal of Materials Chemistry C*, 13(16), 7996–8005. <https://doi.org/10.1039/D5TC00397K>
10. Ghata, A., Eckert, P. L., Böger, T., Garg, P., & Zeie, W. G. (2025). Influence of  $\text{Cu}^+$  Substitution on the Structural, Ionic, and Thermal Transport Properties of  $\text{Ag}_{8-x}\text{Cu}_x\text{GeS}_6$  Argyrodites. *Chemistry of Materials*, 37(17), 6900–6911. <https://doi.org/10.1021/acs.chemmater.5c01679>
11. Gorochoy, O. (1968). Les composés  $\text{Ag}_8\text{MX}_6$  (M= Si, Ge, Sn et X= S, Se, Te). *Bulletin de la Société Chimique de France*, 101, 2263–2275.
12. Heep, B. K., Weldert, K. S., Krysiak, Y., Day, T. W. Zeier, W. G., Kolb U., Snyder, G. J., & Tremel, W. (2017). High electron mobility and disorder induced by silver ion migration lead to good thermoelectric performance in the argyrodite  $\text{Ag}_8\text{SiSe}_6$ . *Chemistry of Materials*, 29(11), 4833–4839. <https://doi.org/10.1021/acs.chemmater.7b00767>
13. Hofmann, A. M. (1988). Silver-Selenium-Silicon, Ternary Alloys. *VCH*, 2, 559–560.

14. Huseynova, I. F., Bayramova, N. A., Imamalieva, S. Z., Aliyeva, A. Sh., Yusibov, Yu. A., & Babanly, M. B. (2025). Phase equilibria in the  $\text{Ag}_8\text{GeSe}_6\text{-Ag}_7\text{GeSe}_5\text{-GeSe}_2$  system. *Russian Journal of Inorganic Chemistry*, 70(11), 1793–1802.
15. Ismayilova, E. N., Huseynova, I. F., Mashadiyeva, L. F. Bakhtiyarly, I. B., & Gasymov, V. A. (2025). Experimental study of phase equilibria in the  $\text{Cu}_2\text{SnSe}_3\text{-Cu}_3\text{SbSe}_4\text{-Se}$  ternary system. *Condensed Matter and Interphases*, 27, 606–614.
16. Ismayilova, E. N., Mashadiyeva, L. F., & Balajayeva, A. N. (2021). Phase equilibria along the  $\text{Cu}_3\text{SbSe}_4\text{-GeSe}_2$  section of the  $\text{Cu-Ge-Sb-Se}$  system New Materials. *Compounds and Applications*, 5(1), 52–58.
17. Jiang, Q., Li, S., Luo, Y., et al. (2020). Ecofriendly highly robust  $\text{Ag}_8\text{SiSe}_6$ -based thermoelectric composites with excellent performance near room temperature. *ACS Applied Materials & Interfaces*, 12(49), 54653–54661. <https://doi.org/10.1021/acsami.0c15877>
18. Kang, T., Li, Ch., Zhang, X., Nakamura, Y., Tseng, J.-Ch., Manjo, T., Liu Ch., & Yang, L. (2026). Local Symmetry Breaking Induced Superionic Conductivity in Argyrodites. *Journal of the American Chemical Society*, 148(6), 6158–6166. <https://doi.org/10.1021/jacs.5c17193>
19. Khan, M. E., & Aslam, J. (2023). *Metal-Chalcogenide Nanocomposites. Fundamentals, Properties and Industrial Applications*. Woodhead Publishing.
20. Krebs, B., & Mandt, J. (1977). Zur Kenntnis des Argyrodit-Strukturtyps: die Kristallstruktur von  $\text{Ag}_8\text{SiSe}_6$ . *Zeitschrift für Naturforschung B: A Journal of Chemical Sciences*, 32, 373–379.
21. Kuhs, W. F. R., & Scheunemann, N. K. (1979). The argyrodites — A new family of tetrahedrally close-packed structures. *Materials Research Bulletin*, 14, 241–248. [https://doi.org/10.1016/0025-5408\(79\)90125-9](https://doi.org/10.1016/0025-5408(79)90125-9)
22. Li, N.-H., Zhang, Q., Shi, X.-L., Jiang, J., & Chen, Z.-G. (2024). Silver Copper Chalcogenide Thermoelectrics: Advance, Controversy, and Perspective. *Advanced materials*, 35(37), 2313146. <https://doi.org/10.1002/adma.202313146>
23. Lin, S., Hou, Y., Yang, J., & Fan, P. (2024). Enhanced Weighted Mobility Induced High Thermoelectric Performance in Argyrodite  $\text{Ag}_8\text{SnSe}_6$ . *ACS Applied Materials & Interfaces*, 16(43), 58912–58919. <https://doi.org/10.1021/acsami.4c14311>
24. Parashchuk, T., Cherniushok, O., Wiendlocha, B., Tobola, J., Cardoso-Gil, R., Snyder, G.J., Grin Y., & Wojciechowski K. T. (2025). High Thermoelectric Performance in Low-Cost  $\text{Cu}_8\text{Si}_x\text{Se}_{6-x}$  Argyrodite. *Advanced functional materials*, 35(34), 2502163. <https://doi.org/10.1002/adfm.202502163>
25. Piskach, L. V., Parasyuk, O. V., Olekseyuk, I. D., Romanyuk, Y. E., Volkov, S. V., & Pekhnyo, V. I. (2006). Interaction of argyrodite family compounds with the chalcogenides of II-b elements. *Journal of Alloys and Compounds*, 421(1-2), 98–104. <https://doi.org/10.1016/j.jallcom.2005.11.056>
26. Poladova, A. N., Huseynova, I. F., Alverdiyev, I. J., Gasymov, V. A., Mashadiyeva, L. F., & Babanly, M. B. (2025).  $\text{Cu}_8\text{GeSe}_6\text{-Ag}_8\text{GeSe}_6$  System: Phase Equilibria and High-Entropy Alloys. *Russian Journal of Inorganic Chemistry*, 70(11), 1778–1784.
27. Portniagin, A. S., Karamysheva, S. P., Bogdanov, K. V., Ushakova, E. V., & Rogach, A. L. (2025). Interplay between the shape anisotropy and optical properties of Cu- and Ag-based ternary and quaternary chalcogenide nanocrystals. *Nanoscale*, 17, 16193–16212. <https://doi.org/10.1039/D5NR01376C>
28. Puthran, S., Hegde, G. Sh., & Prabhu, A. N. (2024). Review of Chalcogenide-Based Materials for Low-, Mid-, and High-Temperature Thermoelectric Applications. *Journal of Electronic Materials*, 53, 5739–5768. <https://doi.org/10.1007/s11664-024-11310-7>
29. Ren, Q., Gupta, M. K., Jin, M., Ding, J., & Wu, J. (2023). Extreme phonon anharmonicity underpins superionic diffusion and ultralow thermal conductivity in argyrodite  $\text{Ag}_8\text{SnSe}_6$ . *Nature Materials*, 22, 999–1006. <https://doi.org/10.1038/s41563-023-01560-x>
30. Shen, X., Koza, M. M., Tung, Y.-H., Ouyang, N., Yang, C.-C., Wang, C., Chen, Y., Willa, K., Heid, R., Zhou, X., & Weber, F. (2023). Soft Phonon Mode Triggering Fast Ag Diffusion in Superionic Argyrodite  $\text{Ag}_8\text{GeSe}_6$ . *Small*, 19(49), 2305048.

<https://doi.org/10.1002/sml.202305048>

31. Studenyak, I. P., Pogodin, A. I., Studenyak, V. I., Izai, V. Y., Filep, M. J., Kokhan, O. P., & Kúš, P. (2020). Electrical properties of copper- and silver-containing superionic  $(\text{Cu}_{1-x}\text{Ag}_x)_7\text{Si}_5\text{I}$  mixed crystals with argyrodite structure. *Solid State Ionics*, 345, 115183. <https://doi.org/10.1016/j.ssi.2019.115183>
32. Venkatraman, M., Blachnik, R., & Schlieper, A. (1995). The phase diagrams of  $\text{M}_2\text{X}-\text{SiX}_2$  (M is Cu, Ag; X is S, Se). *Thermochimica Acta*, 249, 13–20. [https://doi.org/10.1016/0040-6031\(95\)90666-5](https://doi.org/10.1016/0040-6031(95)90666-5)
33. Wang, B., Li, S., Luo, Y., Yang, J., Ye, H., Liu, Y., & Jiang, Q. (2024). A new thermoelectric  $\text{Ag}_8\text{SiSe}_6$  argyrodite for room temperature application: sensitivity of thermoelectric performance to cooling conditions. *Materials Advances*, 5(9), 3735–3741.
34. Wei, P.-Ch., Hsing, Ch.-R., Yang, Ch.-Ch., Tung, Y.-H. et al. (2024). Liquid-like thermal conductivity in solid materials: Dynamic behavior of silver ions in argyrodites. *Nano energy*, 122, 109324. <https://doi.org/10.1016/j.nanoen.2024.109324>